



## Low-weight and UAV-based Hyperspectral Full-frame Cameras for Monitoring Crops: Spectral Comparison with Portable Spectroradiometer Measurements

GEORG BARETH, HELGE AASEN, JULIANE BENDIG, Köln, MARTIN LEON GNYP, Dülmen, ANDREAS BOLTEN, Köln, ANDRÁS JUNG, Leipzig, RENÉ MICHELS, Ulm & JUSSI SOUKKAMÄKI, Oulu, Finland

**Keywords:** UAV, sensors, hyperspectral, change detection, agriculture, CSM, plant height, 3D, vegetation index, crops

**Summary:** The non-destructive monitoring of crop growth status with field-based or tractor-based multi- or hyperspectral sensors is a common practice in precision agriculture. The demand is given for flexible, easy to use, and field scale systems with super-high resolution ( $< 20$  cm) or on single plant scale to provide knowledge on in-field variability of crop status for management purposes. Satellite- and airborne systems are usually not able to provide the spatial and temporal resolution for such purposes within a low-cost approach. The developments in the area of Unmanned Aerial Vehicles (UAV) equipped with hyperspectral sensor systems may be suited to fill that niche. In this contribution, we introduce two hyperspectral full-frame cameras weighing less than 1 kg which can be mounted to low-weight UAVs ( $< 3$  kg). The first results of a campaign in June/July 2013 are presented and the derived spectra from the hyperspectral images are compared to related spectra collected with a portable spectroradiometer. The first results are promising.

**Zusammenfassung:** Leichte und UAV-getragene hyperspektrale, bildgebende Kameras zur Beobachtung von landwirtschaftlichen Pflanzenbeständen: spektraler Vergleich mit einem tragbaren Feldspektrometer. Die nicht-destruktive Beobachtung von Pflanzenwachstum mit feldbasierten oder traktorbasierten multi- oder hyperspektralen Sensoren ist eine gängige Praxis in der Präzisionslandwirtschaft. Um Wissen über die Variabilität des Pflanzenzustands im Feld für Managementzwecke bereitzustellen, werden flexible, multitemporal einsetzbare und einfach zu bedienende Systeme zur Erfassung ganzer Felder mit extrem hoher Auflösung ( $< 20$  cm) oder für Einzelpflanzen benötigt. Satelliten- und flugzeuggetragene Systeme sind in der Regel nicht in der Lage, diese räumliche und zeitliche Auflösung für solche Anwendungen bereitzustellen, bzw. dies wäre mit einem nicht vertretbaren finanziellen Aufwand verbunden. Die Entwicklungen im Bereich der Unmanned Aerial Vehicles (UAV) sowie der hyperspektralen Sensortechnik scheinen genau diese Nische zu füllen. In diesem Beitrag stellen wir zwei hyperspektrale Kameras mit einem Gewicht von weniger als 1 kg vor, die mit leichten UAVs ( $< 3$  kg) geflogen werden können. Wir präsentieren die ersten Ergebnisse einer Kampagne im Juni/Juli 2013 und vergleichen die aus den hyperspektralen Bildern abgeleiteten Spektren mit entsprechenden Spektren eines tragbaren Feldspektrometers. Die ersten Ergebnisse sind vielversprechend.

## 1 Introduction

In Precision Agriculture (PreAg), sensor-based monitoring of crops to derive plant growth parameters and yield are in the focus of research to support proper crop management (MULLA 2013). Therefore, the applications of remote and proximal sensing methods are key technologies in PreAg (OERKE et al. 2010). Besides monitoring crops, sensing technologies are also widely used for measuring soil and environmental parameters (WHELAN & TAYLOR 2013). Hyperspectral remote and proximal sensing is intensively investigated for the detection of crop nitrogen (N) content, biomass, yield and crop stress (KOPPE et al. 2012, LI et al. 2010, OERKE et al. 2010, THENKABAIL et al. 2000, YU et al. 2013). In general, the remote sensing approaches described in the literature are satellite- or airborne (manned airplanes). For proximal sensing approaches, portable field spectrometer are used for canopy or leaf-level sensing (GNYP et al. 2014, YU et al. 2013). In the last years, efforts have been undertaken to make hyperspectral data more frequently available and sensing methods for a specific crop growth stage were investigated (AASEN et al. 2014, GNYP et al. 2013). The latter is a precondition for monitoring plant growth behaviour by multi-temporal campaigns during phenology which enables the detection of abiotic and biotic stresses (LAUDIEN & BARETH 2006, LAUDIEN et al. 2006).

For the consideration of specific phenological stages in non-destructive sensing approaches, a very flexible platform is needed. Usually, satellite- or airborne sensors cannot provide such multitemporal data within a fixed time slot of a few days (ZHANG & KOVACS 2012). Besides the demand for high temporal resolution in crop monitoring approaches, a high spatial resolution is in the focus of PreAg resulting in increased knowledge on within-field variability of crop growth. Unmanned aerial vehicles (UAVs) also known as unmanned aerial systems (UAS) or remotely-piloted aerial systems (RPAS) are remote sensing platforms combining very high flexibility in temporal scale and very high resolution in spatial scale (ZHANG & KOVACS 2012). The potential of UAV-based imaging in agricultural applications is already well described

by ZHANG & KOVACS (2012), CALDERÓN et al. (2013), ZARCO-TEJADA et al. (2012) and others.

The fast technological progress and developments are not only found for UAV platforms, but also for sensor development (BARETH et al. 2011, BENDIG & BARETH 2014). Electronic devices were continuously minimized in the last years which resulted in low-weight sensors being very capable for the integration in small remote sensing platforms (COLOMINA & MOLINA 2014). Hence, in 2013 two new hyperspectral, full-frame imaging spectrometers were introduced, the Cubert UHD185 “Firefly” ([www.cubert-gmbh.de](http://www.cubert-gmbh.de)) and the Rikola hyperspectral camera ([www.rikola.fi](http://www.rikola.fi)), and in 2014 the BaySpec OCI-1000 ([www.bayspec.com](http://www.bayspec.com)). All three low-weight (< 1 kg) cameras cover the spectral VIS/NIR domain but use different technologies. The Rikola and the Cubert sensors were flown in a first campaign in June/July 2013. The objectives of this contribution are (i) to introduce the two hyperspectral frame cameras, which document a new milestone in hyperspectral imaging spectroscopy, and (ii) to compare spectra from the images acquired by UAV-campaigns on barley field experiments with spectra measured with the fieldspectroradiometer FieldSpec3 by ASDI ([www.asdi.com](http://www.asdi.com)).

## 2 Study Area, UAV, and Sensors

The field experiment is located on the research farm of Bonn University, called Campus Klein-Altendorf, which is outside of the city of Bonn in Rheinbach. The field campaigns were carried out within the Crop.Sense.net project’s activity, coordinated by the Institute of Crop Science and Resource Conservation of Bonn University ([www.cropsense.de](http://www.cropsense.de)). Crop.Sense.net is one of the BMBF Networks of Excellence in Agricultural and Nutrition Research, which are funded by the German Ministry for Education and Research (BMBF) and by the European Union Funds for regional development. In Klein-Altendorf, the central field experiments of Crop.Sense.net for barley and sugar beet have been conducted. For this study, multi-temporal UAV campaigns were flown over barley in 2013. The experiment covers 36 plots (each 3 by 7 m) with 18 barley

varieties and two nitrogen treatments (40 and 80 kg/ha). For this first spectral comparison and evaluation, only selected plots (plot numbers 41, 42, and 43) are investigated.

For the UAV campaigns, a HiSystems MK Oktokopter was flown which is a low-cost (<2000 €) and low-weight UAV (<1.5 kg). The latter is an important fact due to the aviation regulations in Germany which al-



**Fig. 1:** Top: MK Oktokopter is prepared for a flight campaign with the Rikola hyperspectral camera, middle: Cubert UHD185 Firefly is calibrated against a white panel before take-off, bottom: UHD185 in the air mounted on a MK Oktokopter.

low commercial and non-commercial imaging campaigns with UAVs weighing less than 5 kg. The MK Oktokopter has a payload of up to 1 kg and a flight endurance of approximately 15 min. It can be auto-piloted by using waypoints. The UAV platform is described in detail by BENDIG et al. (2013). Two hyperspectral full-frame cameras were mounted to the UAV and were flown separately after each other over the same experimental fields. In Fig. 1 (top), the MK Oktokopter is shown before take-off with the mounted Rikola hyperspectral camera (RHC), which is based on Piezo-Actuated Fabry-Perot Interferometer (FPI) (MÄKELÄINEN et al. 2013). FPI enables tunable wavelength settings resulting in a time lag for each wavelength (MÄKELÄINEN et al. 2013). The wavelength is produced by a tunable air gap (vacuum) between two optical layers (HONKAVAARA et al. 2013). Therefore, the spectral wavelength is a function of the size of the air gap. The tuning of the air gap results in an individual image acquisition for each spectral band with a CMOSIS CMOS image sensor recording 1 megapixel (MÄKELÄINEN et al. 2013). The RHC covers the spectral region between 400 nm to 950 nm. Before take-off, the RHC can be calibrated against a white reference panel. The images are saved onboard on a SD card.

The Cubert UHD185 Firefly is designed and developed by the Institute of Laser Technologies in Medicine and Metrology at the University of Ulm and the Cubert GmbH, Germany. The camera records hyperspectral full-frames with 137 bands in a spectral range of 450 nm – 950 nm. A silicon CCD chip captures an image with 1000 by 970 grayscale pixels as well as 50 by 50 hyperspectral pixels. At a flying altitude of 30 m the grayscale image has a ground resolution of about 1 cm and a pure hyperspectral ground resolution of about 20 cm. However, the latter may be pan-sharpened by the software of the manufacturer to the resolution of the grayscale image. The footprint of each scene at 30 m sensor to canopy distance is about 10.3 m. In Fig. 1 (bottom), the UAV-mounted UHD185 is shown. As the RHC, the UHD185 may be calibrated against a white reference panel (Fig. 1, middle). The typical integration time to capture a full hyperspectral data cube is 1 ms (clear sky). The UHD185

has to be flown with a mini-computer (MC) which records the data. Additionally, the MC runs the server application by which the camera can be remotely controlled via WiFi.

The two cameras are differently remote controlled during flight with an UAV. While the measurement of the RHD is controlled by an initialization file which has to be created before the flight, the UHD185 is controlled by the mini-pc with a server application, which may be configured and controlled through WiFi. Depending on the user's needs one of the systems might be beneficial. Additionally, both interfaces are currently still under development and thus, will not be further presented here.

For ground truth data collection, destructive samplings of biomass, plant N- and chlorophyll content, and non-destructive samplings of plant height, hyperspectral, and fluorescence data were performed. Those samplings were continuously carried out during phenology. Canopy reflectance was measured in the barley experiment in 2013 with an ASDI FieldSpec3 Pro (Analytical Spectral Devices, Inc., Boulder, CO, USA). The FieldSpec3 (FS3) measures the reflectance between 350 nm and 2500 nm with a sampling interval of 1.4 nm in the visible near infrared (VNIR) domain and with 2 nm in the shortwave infrared (SWIR) spectral region. The reflectance was measured at a height of 0.5 m above canopy without a fore optic resulting in a 25° field of view to minimize the background signals of soil (Fig. 2). FieldSpec3 campaigns were conducted between 11 am and 2 pm local mean time around solar noon. A condition for the



**Fig. 2:** Sampling hyperspectral ground truth with an ASD FieldSpec3.

measurements is a mostly cloudless sky. A white spectralon panel was used for continuous calibrations. The same reference panel was also used for the RHC and UHD185 calibration (compare Fig. 1, middle). For each plot, a total of six to eight FieldSpec3 spectra were randomly taken to represent a mean plot reflectance.

### 3 Spectral Comparisons

The first UAV campaigns with the UHD185 and the RHC were carried out on June 14<sup>th</sup>, 2013 (Fig. 3). Both hyperspectral frame imagers operated successfully in the air after mounting them to the MK Oktokopter. To compare the spectral results for both camera systems with the FS3 spectra, images were taken at 30 m above ground level covering a maximum of three plots per image. The spatial resolution is as stated above.

Directly after the UAV-based image acquisition the hyperspectral field measurements were taken. For each plot, ten measurements of the FS3 were averaged at six to eight positions (Fig. 4). The measurements were taken from the core of the plots to exclude border effects. The spectra were then averaged to represent the plot's mean reflectance. In Fig. 3, a false colour image of the UHD185 data is dis-

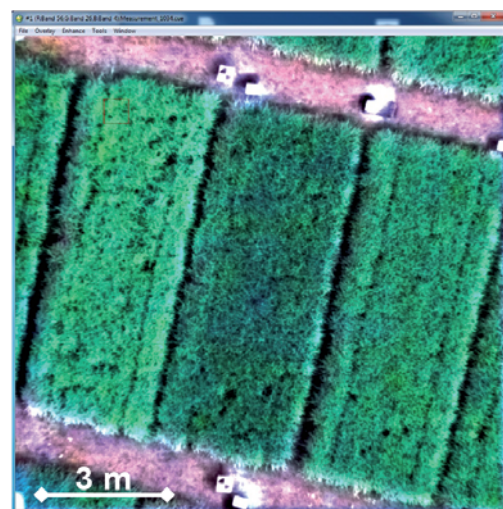


**Fig. 3:** RGB image with the UHD185 covering three barley plots (3 by 7 m each), June 14<sup>th</sup>, 2013.

played. The potential locations of the six FS3 measurements are shown in Fig. 4.

For retrieving the mean plot spectra of the hyperspectral images, polygons with an inner buffer of 0.3 m were digitized to reduce border effects. Spatial statistics were computed for all pixels within a plot polygon to derive mean spectra. In Fig. 5, the polygons are visualized for the three plots, each covering approximately 130,000 pixels of the UHD185 hyperspectral image.

While the polygons in Fig. 5 represent the true area for calculating the spatial statistics, the circles of the single hyperspectral field measurements shown in Fig. 4 do not represent the true location. The latter were captured as shown in Fig. 2 but the locations were randomly selected excluding areas of destructive biomass sampling.

The mean spectra from the UHD185 image shown in Fig. 5 and the corresponding mean spectra from FS3 are plotted in Fig. 6. The

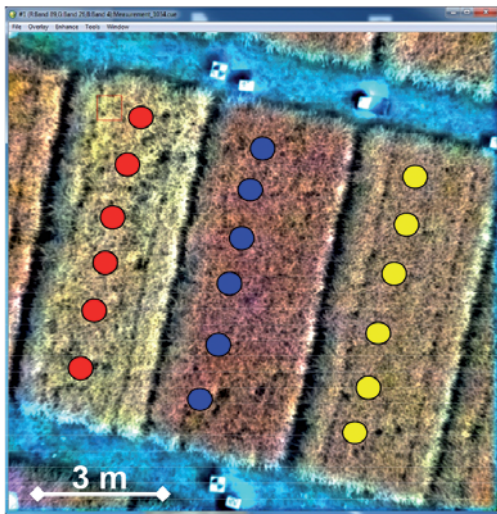


**Fig. 4:** Six randomized FieldSpec3 spectra were taken for each plot on June 14<sup>th</sup>, 2013.

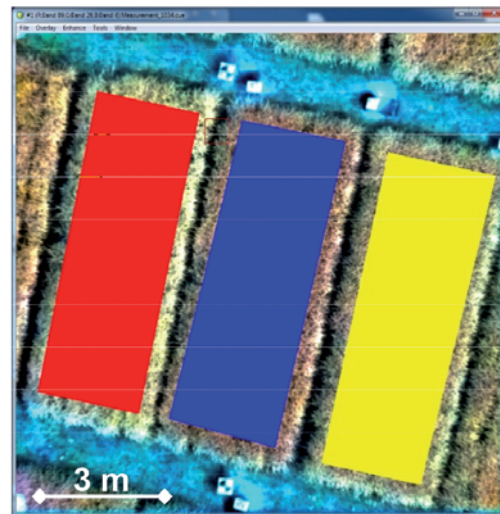


**Fig. 5:** Digitized polygons to calculate spatial statistics for each plot from UHD185 hyperspectral image for June 14<sup>th</sup>, 2013.

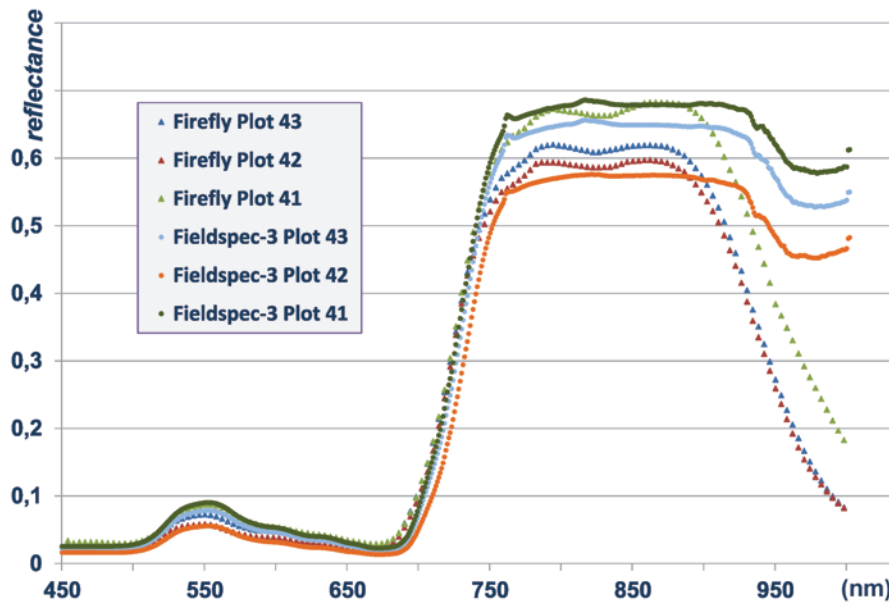


**Fig. 6:** FieldSpec3 spectra vs UHD185 spectra for plots 41, 42, and 43 on June 14<sup>th</sup> 2013.

lines with the denser dotted points represent the FS3 data with higher spectral resolution compared to the UHD185 data with a lower spectral resolution. The magnitude of reflectance is similar and corresponds well. However, in the NIR, differences in the shape of the spectra are visible. Additionally, a decline of reflection in the UHD185 spectra is obvious for wavelengths longer than 900 nm.

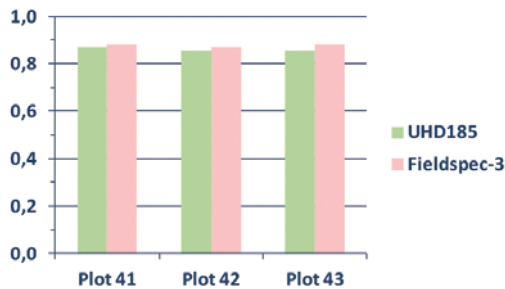


**Fig. 7:** OSAVI for the investigated plots from FieldSpec3 and UHD185 spectra for June 14<sup>th</sup>, 2013.

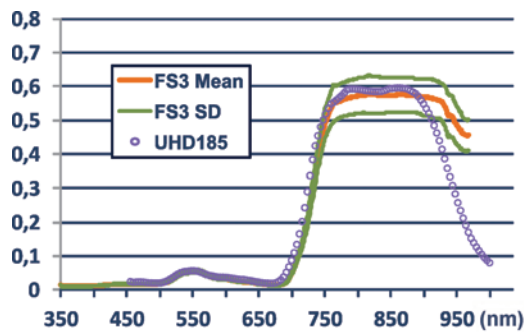


**Fig. 8:** Mean FieldSpec3 spectrum for plot 42 with standard deviation (SD) and mean UHD185 spectrum for June 14<sup>th</sup>, 2013.

To get an impression of the usability of the sensors for vegetation indices (VIs) two common vegetation indices, the optimized soil-adjusted vegetation index (OSAVI) and the normalized difference vegetation index (NDVI), were calculated for the FS3 and UHD185. NDVI is widely used in remote sensing while OSAVI reduces the soil background signals (RONDEAUX et al. 1996). The first impression of similar spectral pattern and magnitude are confirmed for NDVI-like VIs. The OSAVI from FS3 data and UHD185 spectra are shown in Fig. 7 for the investigated plots. They do not show a significant difference having UHD185/FS3 OSAVI values of 0.87/0.88, 0.86/0.87, and 0.85/0.88 for plots 41, 42, and 42, respectively. Similar results were produced for NDVI calculations (Fig. 11).

Additionally, the differences in the spectra between the two sensors are partly within the standard deviation (SD) of the FS3 measurements. As an example, the FS3 spectrum with the SD for plot 42 is displayed in Fig. 8. When compared to the UHD185 spectra, it is visible that in the NIR region the instruments are within SD. The latter is not true for the red

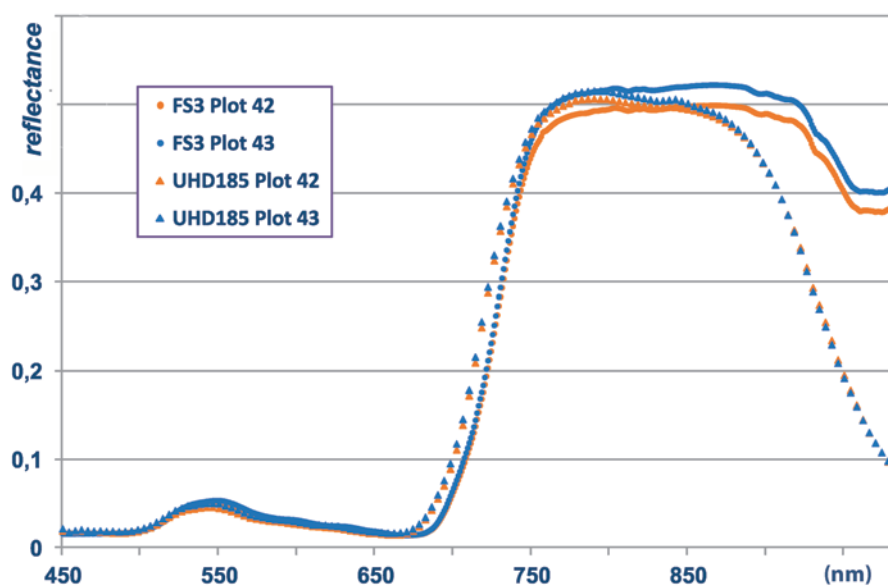


**Fig. 9:** FieldSpec3 and UHD185 spectra for plots 42 and 43 on June 19<sup>th</sup>, 2013.

edge domain and the wavelengths longer than 900 nm. A small spectral shift to the shorter wavelength is observable resulting in large differences when calculating simple ratio VIs from bands in the VIS spectral region.

Similar spectral properties can be described for the UAV campaign with the UHD185 on June 19<sup>th</sup>, 2013 (Fig. 9). In general, lower spectral magnitudes can be observed for plots 42 and 43 in the NIR domain with both sensors while magnitude and overall pattern of the UHD185 fit to the FieldSpec3 measurements. Plot 41 was not investigated due to insufficient coverage. Additionally, the aforementioned shift of the UHD185 occurs again in the red edge domain towards shorter wavelength and the performance from 900 nm onwards is poor.

Finally, very different spectral patterns occur on July 8<sup>th</sup>, 2013 (Fig. 10). It is clearly visible that the FS3 spectra show a very different NIR pattern due to beginning of senescence. This decrease in reflectance between 750 nm and 800 nm is not captured by the UHD185. Additionally, the spectra show higher differences in the VIS domain while the overall magnitudes are still comparable but much weaker than before. The spectral shift towards shorter wavelength is again a characteristic for the red edge spectral regions and for the poor performance above 900 nm.

The Rikola hyperspectral camera (RHC) operates on a different technology, using a Piezo-Actuated Fabry-Perot interferometer (FPI). In moving sensor platforms, a spatial shift of each spectral band might be the consequence and must be solved by image matching techniques. As described above, the RHC enables imaging of selected wavelengths. According to well described VIs (GNYP et al. 2013, LAUDIEN et al. 2006, LI et al. 2010, Yu et al. 2013), we chose eight wavelengths for the UAV campaign on June 14<sup>th</sup>, 2013: 505 nm, 552 nm, 604 nm, 674 nm, 741 nm, 745 nm, 770 nm, and 803 nm. To calculate VIs from the RHC image we used the same polygon as for the image of the UHD185 (Fig. 5).

The NDVI values calculated from the RHC (Fig. 11) are lower than for the UHD185 and

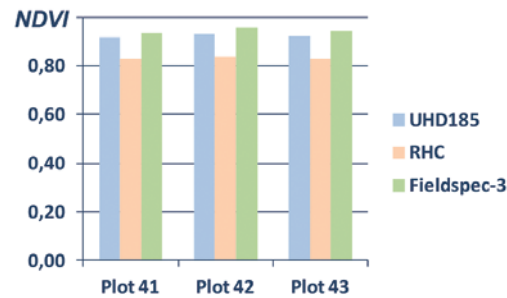


Fig. 11: Calculated NDVI for the investigated plots for June 14<sup>th</sup>, 2013.

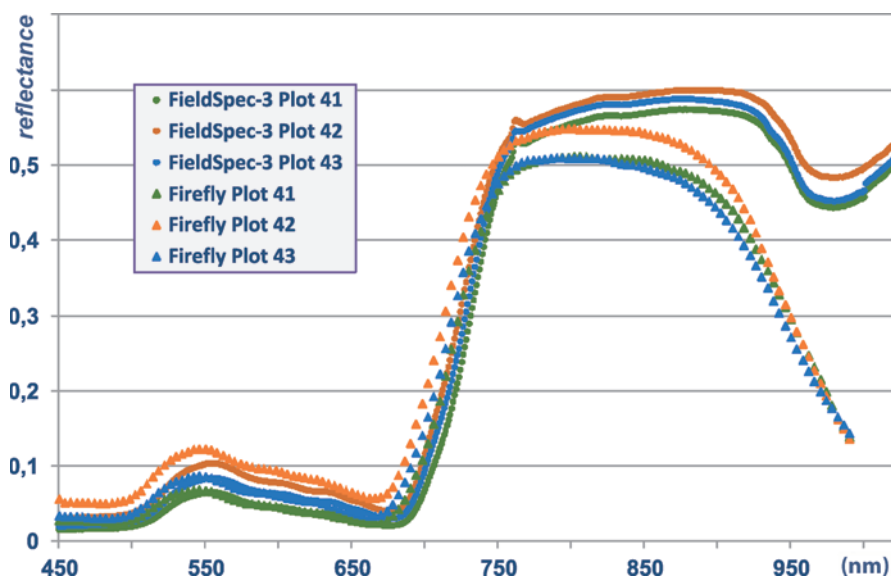
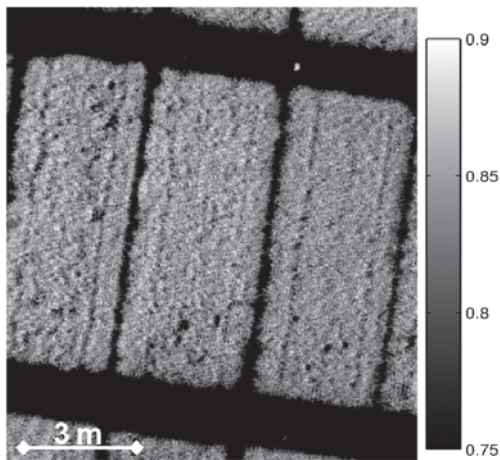


Fig. 10: FieldSpec3 spectra vs. UHD185 spectra for plots 41, 42, and 43 on July 8<sup>th</sup>, 2013.



**Fig. 12:** Calculated NDVI for the RHC image taken on June 14<sup>th</sup>, 2013.

the FS3. The reason for this is not clear at this stage, because the RHC was calibrated against the reference panel, too. But the NDVI values are in an order and pattern as expected and the UHD185 showed weaker performances against the FieldSpec3 measurements on other dates. The higher spatial resolution of the RHC's hyperspectral sensor is documented in the calculated NDVI image shown in Fig.12.

#### 4 Discussion and Conclusions

In this study, we flew the Rikola hyperspectral camera (RHC) and the Cubert UHD185 Firefly with a low-weight and low-cost UAV. Both cameras worked well, had some minor handling problems in the field, and the flight campaigns successfully delivered hyperspectral data. The spectral calibration in the field against a white reference panel was possible for both sensors. While the UHD185 was strong in capturing the whole spectrum within one image, the RHC had a higher spatial resolution in the selected hyperspectral wavelength resulting in a lower spectral resolution. While the RHC was only flown once together with the Rikola company, the UHD185 was flown in multiple campaigns.

For both cameras the spectral calibration is still an issue. While the spectral pattern and magnitudes are in the order of the field measurements, the first comparison with field spectra show clearly a lack of understanding in the

spectral calibration of the sensors. Additionally, the UHD185 and the RHC were flown in different image acquisition modes. Future research of using the two cameras must focus on the hyperspectral image properties in terms of BDRF and calibration. Because of the latter the results stated in this paper should be seen as a first indicator of the suitability of hyperspectral full-frame cameras for precision agriculture applications. Despite the differences between the FS3 measurements and the hyperspectral full-frame sensors in some of the measurements the results show the potential of this new technology. Similar comparison approach between ASD Hand-held 2 and UAV-based sensors, such as Mini MCA6 (Tetracam) and STS spectrometer (Ocean Optics), were performed by VON BUEREN et al. (2014), but only in the spectral domain of 350 nm – 850 nm. The spectra from the different sensors showed similar magnitudes and patterns. However, further research needs to investigate a best practice for full-frame UAV hyperspectral sensors to generate robust and reproducible data. Both sensors operated well in the air and recorded the data as configured. Due to the small field of view of both sensors capturing the right footprint was a challenge. The latter may be solved with improved knowledge of the sensor and optimized flying trajectories.

The new technological designs of both hyperspectral sensors result in a low weight and enable hyperspectral imaging campaigns with UAV at a take-off weight below 5 kg. In Germany, this is important due to aviation regulations, since the application procedure for permissions are easier than for heavier UAVs. Apart from the mentioned critical points, both sensors open a new era of hyperspectral imaging. The flexibility of low-weight UAVs enable a temporal resolution which could not been realized in the past by (manned) aerial- or satelliteborne imaging. The same is true for the spatial resolution. Super-high resolutions of < 2 cm are possible on field scale and up to a few square kilometres, even in 3D (BENDIG et al. 2013). Using stereophotogrammetric or structure for motion image analysis techniques with precise RTK measured ground control points, DEMs or in general surface models can be obtained in a resolution and precision of less than 2 cm. In Fig. 13, such a

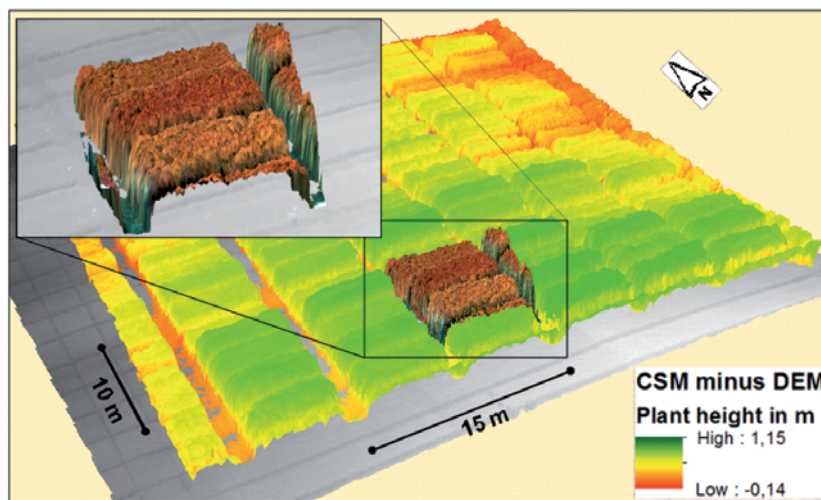


Fig. 13: 3D hyperspectral surface with a spatial resolution of 2 cm.

3D hyperspectral surface is shown for June 14<sup>th</sup>, 2013.

The combination of 3D imaging techniques and hyperspectral imaging enables the precise and accurate monitoring of crop growth during phenology. The analysis of multi-temporal crop surface models (CSM) (BENDIG et al. 2013, TILLY et al. 2014) enables the precise monitoring of plant height and plant growth while hyperspectral analysis derive physiological plant parameters like chlorophyll or nitrogen content and others. Exactly this is needed for PreAg in terms of monitoring crop growth behaviour, crop vitality, and crop stress. The first data analyses are very promising and can be regarded as a new technological statement of sensor development, which will be a multiplier for applications not only in the field of crop monitoring.

### Acknowledgements

The authors acknowledge the funding of the CROP.SENSE.net project in the context of Ziel 2-Programms NRW 2007–2013 “Regionale Wettbewerbsfähigkeit und Beschäftigung (EFRE)” by the Ministry for Innovation, Science and Research (MIWF) of the state North Rhine Westphalia (NRW) and European Union Funds for regional development (EFRE) (005-1103-0018).

### References

- AASEN, H., GNYP, M.L., MIAO, Y. & BARETH, G., 2014: Automated hyperspectral vegetation index retrieval from multiple correlation matrices with HyperCor. – *Photogrammetric Engineering & Remote Sensing* **80** (8): 785–795.
- BARETH, G., BENDIG, J. & BOLTEN, A., 2011: Potentials of low-cost Mini-UAVs. – LENZ-WIEDEMANN, V.I.S. & BARETH, G. (eds.): *Workshop on Remote Sensing Methods for Change Detection and Process Modelling*. – *Kölner Geographische Arbeiten* **92**: 1–8.
- BENDIG, J., BOLTEN, A. & BARETH, G., 2013: UAV-based Imaging for Multi-Temporal, very high Resolution Crop Surface Models to monitor Crop Growth Variability. – *PGF – Photogrammetrie, Fernerkundung, Geoinformation* **2013** (6): 551–562.
- BENDIG, J. & BARETH, G., 2014: Preface. – BENDIG, J. & BARETH, G. (eds.): *Workshop on UAV-based Remote Sensing Methods for Monitoring Vegetation*. – *Kölner Geographische Arbeiten* **94**: 1–2.
- CALDERÓN, R., NAVAS-CORTÉS, J.A., LUCENA, C. & ZARCO-TEJADA, P.J., 2013: High-resolution airborne hyperspectral and thermal imagery for early detection of Verticillium wilt of olive using fluorescence, temperature and narrow-band spectral indices. – *Remote Sensing of Environment* **139**: 231–245.
- COLOMINA, I. & MOLINA, P., 2014: Unmanned aerial systems for photogrammetry and remote sensing: A review. – *ISPRS Journal of Photogrammetry and Remote Sensing* **95**: 79–97.

- GNYP, M.L., YU, K., AASEN, H., YAO, Y., HUANG, S., MIAO, Y. & BARETH, G., 2013: Analysis of crop reflectance for estimating biomass in rice canopies at different phenological stages. – *PGF – Photogrammetrie, Fernerkundung, Geoinformation* **2013** (4): 351–365.
- GNYP, M.L., MIAO, Y., YUAN, F., USTIN, S.L., YU, K., YAO, Y., HUANG, S. & BARETH, G., 2014: Hyperspectral canopy sensing of paddy rice above-ground biomass at different growth stages. – *Field Crops Research* **155**: 42–55.
- HONKAVAARA, E., SAARI, H., KAIVOSOJA, J., PÖLÖNEN, I., HAKALA, T., LITKEY, P., MÄKYNEN, J. & PESSONEN, L., 2013: Processing and Assessment of Spectrometric, Stereoscopic Imagery Collected Using a Lightweight UAV Spectral Camera for Precision Agriculture. – *Remote Sensing* **5**: 5006–5039.
- KOPPE, W., GNYP, M.L., HENNIG, S., LI, F., MIAO, Y., CHEN, X., JIA, L. & BARETH, G., 2012: Multi-temporal hyperspectral and radar remote sensing for estimating winter wheat biomass in the North China Plain. – *PGF – Photogrammetrie, Fernerkundung, Geoinformation* **2012** (3): 281–298.
- LAUDIEN, R. & BARETH, G., 2006: Multitemporal hyperspectral data analysis for regional detection of plant diseases by using a tractor- and an airborne-based spectrometer. – *PGF – Photogrammetrie, Fernerkundung, Geoinformation* **2006** (3): 217–227.
- LAUDIEN, R., BÜRCKY, K., DOLUSCHITZ, R. & BARETH, G., 2006: Aufbau einer webgestützten Spektrallbibliothek zur Analyse hyperspektraler Daten von mit *Rhizoctonia solani* inokulierten Zuckerrüben (Establishment of a web-based spectral database for the analysis of hyperspectral data from *Rhizoctonia solani*-inoculated sugar beet). – *Sugar Industry (Zuckerindustrie)* **131** (56): 164–170.
- LI, F., MIAO, Y., CHEN, X., ZHANG, F., JIA, L. & BARETH, G., 2010: Estimating winter wheat biomass and nitrogen status using an active crop sensor. – *Intelligent Automation and Soft Computing* **16** (6): 1219–1228.
- MÄKELÄINEN, A., SAARI, H., HIPPI, I., SARKEALA, J. & SOUKKAMÄKI, J., 2013: 2D Hyperspectral frame imager camera data in photogrammetric mosaicking. – *International Archives of the Photogrammetry, Remote Sensing and Spatial Information Sciences* **XL-1/W2**: 263–267.
- MULLA, D.J., 2013: Twenty five years of remote sensing in precision agriculture: Key advances and remaining knowledge gaps. – *Biosystems Engineering* **114**: 358–371.
- OERKE, E.C., GERHARDS, R., MENZ, G. & SIKORA, R.A. (eds.), 2010: Precision crop protection – the challenge and use of heterogeneity. – 441 pp., Springer, Dordrecht, The Netherlands.
- RONDEAUX, G., STEVEN, M. & BARET, F., 1996: Optimization of soil-adjusted vegetation indices. – *Remote Sensing of Environment* **55**: 95–107.
- TILLY, N., HOFFMEISTER, D., CIAO, Q., HUANG, S., MIAO, Y., LENZ-WIEDEMANN, V. & BARETH, G., 2014: Multi-temporal Crop Surface Models: Accurate plant height measurement and biomass estimation with terrestrial laser scanning in paddy rice. – *Journal of Applied Remote Sensing* **8** (1): 083671.
- THENKABAIL, P.S., LYON, J.G. & HUETE, A., 2011: *Hyperspectral Remote Sensing of Vegetation*. – 705 pp., CRC Press, FL, USA.
- THENKABAIL, P.S., SMITH, R.B. & PAUW, E.D., 2000: Hyperspectral vegetation indices and their relationship with agricultural crop characteristics. – *Remote Sensing of Environment* **71** (2): 152–182.
- VON BUEREN, S., BURKART, A., HUE NI, A., RASCHER, U., TUOHY, M. & YULE, I., 2014: Comparative validation of UAV based sensors for the use in vegetation monitoring. – *Biogeosciences Discussions* **11**: 3837–3864.
- WHELAN, B. & TAYLOR, J., 2013: *Precision agriculture for grain production systems*. – 208 pp., CSIRO Publishing.
- YU, K., LI, F., GNYP, M.L., MIAO, Y., BARETH, G. & CHEN, X., 2013: Remotely detecting canopy nitrogen concentration and uptake of paddy rice in the Northeast China Plain. – *ISPRS Journal of Photogrammetry and Remote Sensing* **78**: 102–115.
- ZARCO-TEJADA, P.J., GONZÁLES-DUGO, V. & BERNI, J.A.J., 2012: Fluorescence, temperature and narrow-band indices acquired from a UAV platform for water stress detection using a micro-hyperspectral imager and a thermal camera. – *Remote Sensing Environment* **117**: 322–337.
- ZHANG, C. & KOVACS, J.M., 2012: The application of small unmanned aerial systems for precision agriculture: a review. – *Precision Agriculture* **13**: 693–712.

#### Address of the Authors:

Prof. Dr. GEORG BARETH, HELGE AASEN, JULIANE BENDIG & Dr. ANDREAS BOLTEN, University of Cologne, Institute of Geography, GIS & RS Group, Albertus-Magnus-Platz, D-50923 Köln, Tel.: +49-221-470-6265, Fax: +49-221-470-8838, e-mail: {juliane.bendig}, {andreas.bolten}, {g.bareth}@uni-koeln.de

Dr. MARTIN LEON GNYP, Research Centre Hanninghof, Yara International, c/o Yara GmbH & Co KG, Hanninghof 35, D-48249 Dülmen, Tel.: +49-2594-

798-196, Fax.: +49-2594-7455, e-mail: martin.gnyp@yara.com

Dr. ANDRÁS JUNG, Institute of Geography, University of Leipzig, Johannisallee 19, D-04103 Leipzig, Tel.: +49-341-97-32785, Fax: +49-341-97-32799, e-mail: andras.jung@uni-leipzig.de

Dr. RENÉ MICHELS, Cubert GmbH, Real Time Spectral Imaging, Helmholtzstraße 12, D-89081 Ulm, Tel.: +49-73-11-42-99-97, e-mail: michels@cubert-gmbh.de

JUSSI SOUKKAMÄKI, Rikola LTD., Kaitoväylä 1, FI-90570 Oulu, Finland, Tel.: +358-40-540-8794, e-mail: jussi.soukkamaki@rikola.fi

Manuskript eingereicht: Juli 2014  
Angenommen: September 2014